Journal of Engineering Science and Technology
Vol. 15, No. 4 (2020) 2270 - 2288
© School of Engineering, Taylor's University

OPTIMAL H2PID CONTROLLER DESIGN FOR HUMAN SWING LEG SYSTEM USING CULTURAL ALGORITHM

HAZEM I. ALI, AMJAD F. HASAN*, HAIDER M. JASSIM

Control and System Engineering Department,
University of Technology-Iraq
*Corresponding Author: 60037@uotechnology.edu.iq

Abstract

In this paper, a hybrid controller which combines of two control designs is proposed to control the nonlinear human walking swing leg system (HWSS) by producing a dynamic output feedback. The HWSS is modelled as a double pendulum with nonlinearity, uncertainty and MIMO properties. Therefore, these challenges are considered to verify the effectiveness of the proposed controller. The H_2 state feedback controller and PID controller are fused together to form a new optimal robust controller. The H_2 full state feedback controller is only used in the first control design and the H_2 full state feedback with PID controller are used in the second control design to effectively compensate the system and achieve the desired tracking properties. The cultural algorithm (CA) method, which is one of the effective optimization algorithms, is used to obtain the optimal parameters of the controller. The results show that the proposed H_2PID controller can robustly stabilize the system and achieve a desirable specification, in the presence of uncertainty and disturbance. Finally, it can be seen that the findings of this work show the superiority of the proposed H_2PID controller in that it can overcome the effect of the coupling and achieve the required performance.

Keywords: Cultural algorithm, Double pendulum, Human walking swing leg system (HWSS), Nonlinear-control, Optimal control.

1. Introduction

Leg locomotion represents the most intricate motions in the human leg or in the humanoid robotic leg because of its complicated nonlinear behavior. Therefore, it is required to design a robust controller to achieve the desired tracking performance while coping with the high nonlinearities and parameters uncertainty [1].

The ability of the human to move from one place to another depends on the three prospects of walking, running, and jogging gaits. Walking is the commonly used gait in human movement. It has two prime phases: single support phase (SSP) which is one leg moving (swing) and the other leg will be fixed (stance), and double support phase (DSP) [1]. This research study focuses on the SSP phase because the SSP has much common share in walking gait and it is more interesting than DSP. The swing leg of SSP is usually modelled as a double pendulum. The thigh and shank of the human leg will appear as the links of the double pendulum which are connected by the hip and knee joints. The joints connect the upper part of the thigh with the body and the lower part of the thigh with the shank. Therefore, two motors can replace these joints in an artificial walking system [1]. The human walk is characterized by its stability and the excellent robust muscular control. It is important to mention that the stability and control of one leg will have an impact on the whole body locomotion behavior. A few researchers have modelled the dynamic system of leg locomotion to self-impact double pendulum (SIDP) [2]

The literature is enriched with research contributions addressing the issue of controlling and enhancing the performance of artificial human walking swing leg system (HWSS). The numerical methods, Fourier series approximation and inverse, temporal finite element, and advanced computer based numerical tool were used by Dragnis to find an optimal control for HWSS but the model of HWSS was never made to be more realistic [3]. Zang et al. proposed a Proportional and Derivative controller (PD) to improve the robustness, response speed, position accuracy, and intelligent behavior of the system. The PD controller was used to control the two motors which represented the hip and knee joints. However, the problem was the torques applied by the motors were very high [4]. The Model Predictive Control (MPC) has been suggested by Wang et al. to calculate the torques, angles, and velocities of the joints based on the parameters of the gait. Nevertheless, the disturbance was not completely rejected by the MPC and the control action had unacceptable reaction [5]. A feedback controller based on learned probabilistic which was proposed to generate policies of walking using a very small set of data from scratch. However, the parameters of the controller were not optimal because the cost function lacks the holistic optimal solution of the system [6]. A state feedback controller has been developed by Desai and Geyer, the method utilized the advantage of segment reaction to control leg placement under the effect of large disturbance. However, the results showed that the actual output didn't fit the desired input [7]. An Adaptive Neural Network (ANN) controller was proposed by Bazargan et al. to robustly control the nonlinear human swing leg system. The controller was designed based on an inherently nonlinear ANN which passes through a time-consuming training process to evaluate the inverse dynamic of the model [8]. A Neural Network Predictive Control (NNPC) has been suggested by Ekkachai and Nilkhamhang to control a semi-active prosthetic knee with a constant speed for walking. For this reason, the controller cycle was slowed down to be compliable with the changes in gait since damping constant was increasing in each step [9]. An optimal PID controller using two optimization methods for a biped robot walking has been proposed by Ravi and Pandu in 2019. It was found that the Modified Chaotic Invasive

Weed Optimization (MCIWO) can give a better performance than that of the PSO method [10]. Boxing et al. in 2019 have proposed a multi-module controller for walking quadruped robots. The Central Pattern Generator (CPG) method was used to design the controller [11]. Hazem and Mustafa in 2018 have proposed a mixed H_2/Sliding mode controller for human swing leg system the controller weights parameters have been set manually to give the required performance. The proposed mixed controller has given a performance better than if one of them was used [12].

In this paper, a full state feedback H_2 controller, which is represent one of most popular robust controllers, is integrated with dual PID controllers and optimized together, using Culture Algorithm (CA) to control the HWSS system. The second section of this paper presents the system mathematical modeling while the design procedure for the proposed controller is addressed in the third section. Results and discussion will be provided in section four. Section five is devoted for conclusion.

2. Materials and Methods

The human walking swing system represents the leg system when the hip and knee joints are mobilized while the ankle contribution neglected [13]. The system has been modelled by a double pendulum as shown in Fig. 1. It is clear to see there are two links representing the hip and knee joints that used to connect the thigh with the body (hip joint) and thigh with the shank (knee joint). The mass and length of the thigh are m_1 and l_1 respectively and the mass and length of the shank are m_2 and l_2 respectively. The rotation angles for the hip and knee joint are θ_1 and θ_2 respectively and the external torques applied on the thigh and shank are τ_1 and τ_2 respectively [1, 2, 8].

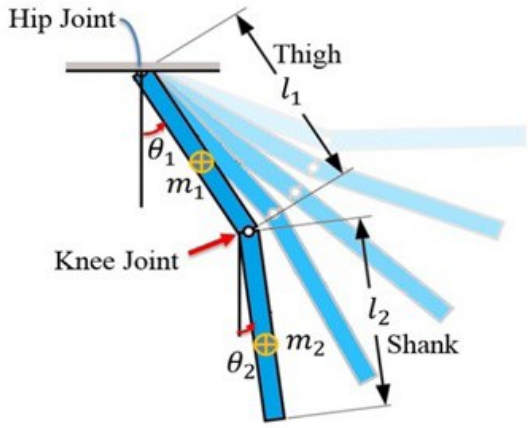

Fig. 1. Schematic of HWSS [8].

The equations of position for the thigh and shank respectively are [14]

$$X_1 = \frac{1}{2} l_1 \sin\theta_1$$
$$Y_1 = \frac{1}{2} l_1 \cos\theta_1 \quad (1)$$
$$X_2 = l_1 \sin\theta_1 + \frac{1}{2} l_2 \sin\theta_2$$

$$Y_2 = l_1 \cos\theta_1 + \frac{1}{2} l_2 \cos\theta_2 \quad (2)$$

The linear velocity for shank is

$$v_2 = \sqrt{\dot{X}_2^2 + \dot{Y}_2^2} \quad (3)$$

By differentiating Eq. (2) and substituting the result in Eq. (3), yields

$$v_2 = \sqrt{\left(l_1 \dot{\theta}_1 \cos\theta_1 + \frac{1}{2} l_2 \dot{\theta}_2 \cos\theta_2\right)^2 + \left(-l_1 \dot{\theta}_1 \sin\theta_1 - \frac{1}{2} l_2 \dot{\theta}_2 \sin\theta_2\right)^2}$$

$$= \sqrt{l_1^2\dot{\theta}_1^2 + l_1\dot{\theta}_1 l_2\dot{\theta}_2 \cos(\theta_1 - \theta_2) + \frac{1}{4} l_2^2 \dot{\theta}_2^2} \quad (4)$$

The kinematic energy is [14, 15]:

$$K_e = \frac{1}{2} I_1 w_1^2 + \frac{1}{2} I_2 w_2^2 + \frac{1}{2} m_2 v_2^2 \quad (5)$$

where $w_1 = \dot{\theta}_1$ $w_2 = \dot{\theta}_2$, $I_1 = \frac{1}{3} m_1 l_1^2$ (thing moment of inertia) and $I_2 = \frac{1}{12} m_2 l_2^2$ (shank moment of inertia)

then

$$K_e = \frac{1}{2}\left(\frac{1}{3} m_1 l_1^2\right)\dot{\theta}_1^2 + \frac{1}{2}\left(\frac{1}{12} m_2 l_2^2\right)\dot{\theta}_2^2 + \frac{1}{2} m_2 \left(l_1^2\dot{\theta}_1^2 + l_1\dot{\theta}_1 l_2\dot{\theta}_2 \cos(\theta_1 - \theta_2) + \frac{1}{4} l_2^2 \dot{\theta}_2^2\right)$$

$$= \frac{1}{6} m_1 l_1^2 \dot{\theta}_1^2 + \frac{1}{6} m_2 l_2^2 \dot{\theta}_2^2 + \frac{1}{2} m_2 \left(l_1^2\dot{\theta}_1^2 + l_1\dot{\theta}_1 l_2\dot{\theta}_2 \cos(\theta_1 - \theta_2)\right) \quad (6)$$

The potential energy of the system is [14, 15]:

$$P_e = m_1 g h_1 + m_2 g h_2$$

$$= -\frac{1}{2} m_1 g l_1 \cos\theta_1 - m_2 g \left(l_1 \cos\theta_1 + \frac{1}{2} l_2 \cos\theta_2\right) \quad (7)$$

where h_1 and h_2 represent the heights of the center mass for thigh and shank respectively, and g is the acceleration of gravity.

By using Lagrange Dynamics [15]

$$L = K_e + P_e \quad (8)$$

and by substituting Eqs. (6) and (7) in Eq. (8), yields

$$L = \frac{1}{6} m_1 l_1^2 \dot{\theta}_1^2 + \frac{1}{6} m_2 l_2^2 \dot{\theta}_2^2 + \frac{1}{2} m_2 \left(l_1^2\dot{\theta}_1^2 + l_1\dot{\theta}_1 l_2\dot{\theta}_2 \cos(\theta_1 - \theta_2)\right) + \left(\frac{1}{2} m_1 + m_2\right) g l_1 \cos\theta_1 + \frac{1}{2} m_2 g l_2 \cos\theta_2 \quad (9)$$

The equation of Euler-Lagrange [15]

$$\frac{d}{dt}\left[\frac{\partial L}{\partial \dot{\theta}_i}\right] - \frac{\partial L}{\partial \theta_i} = \tau_i \quad (10)$$

where $i = 1,2$

then

$$\frac{\partial L}{\partial \dot{\theta}_1} = \left(\frac{1}{3} m_1 + m_2\right) l_1^2 \dot{\theta}_1^2 + \frac{1}{2} m_2 l_1 l_2 \dot{\theta}_2 \cos(\theta_1 - \theta_2) \quad (11)$$

$$\frac{d}{dt}\left[\frac{\partial L}{\partial \dot{\theta}_1}\right] = \left(\frac{1}{3}m_1 + m_2\right) l_1^2\ddot{\theta}_1^2 + \frac{1}{2}m_2 l_1 l_2 \ddot{\theta}_2 \cos(\theta_1 - \theta_2) - \frac{1}{2}m_2 l_1 l_2 \dot{\theta}_2 \sin(\theta_1 - \theta_2)\left(\dot{\theta}_1 - \dot{\theta}_2\right) \quad (12)$$

$$\frac{\partial L}{\partial \theta_1} = -\frac{1}{2}m_2 l_1 l_2 \dot{\theta}_1 \dot{\theta}_2 \sin(\theta_1 - \theta_2) - \left(\frac{1}{2}m_1 + m_2\right) g l_1 \sin\theta_1 \quad (13)$$

and

$$\frac{\partial L}{\partial \dot{\theta}_2} = \frac{1}{3}m_2 l_2^2 \dot{\theta}_2^2 + \frac{1}{2}m_2 l_1 l_2 \dot{\theta}_1 \cos(\theta_1 - \theta_2) \quad (14)$$

$$\frac{d}{dt}\left[\frac{\partial L}{\partial \dot{\theta}_2}\right] = \frac{1}{2}m_2 l_1 l_2 \ddot{\theta}_2^2 \cos(\theta_1 - \theta_2) - \frac{1}{2}m_2 l_1 l_2 \dot{\theta}_1 \sin((\theta_1 - \theta_2)\left(\dot{\theta}_1 - \dot{\theta}_2\right) + \frac{1}{3}m_2 l_2^2 \ddot{\theta}_2 \quad (15)$$

$$\frac{\partial L}{\partial \theta_2} = \frac{1}{2}m_2 l_1 l_2 \dot{\theta}_1 \dot{\theta}_2 \sin(\theta_1 - \theta_2) - \frac{1}{2}m_2 g l_2 \sin\theta_2 \quad (16)$$

Substituting Eqs (12)-(13) and (15) in Eqs (16) and (10), the dynamic equations of the system will be represented by Lagrange's method to be [2, 8, 15].

$$\tau_1 = \frac{(m_1+3m_2)}{2} l_1^2\ddot{\theta}_1 + \frac{m_2 l_1 l_2 \ddot{\theta}_2}{2}\cos(\theta_1 - \theta_2) - \frac{m_2 l_1 l_2 \dot{\theta}_2^2}{2}\sin(\theta_1 - \theta_2) + \frac{(m_1+2m_2)}{2} g l_1 \sin\theta_1 \quad (17)$$

$$\tau_2 = \frac{1}{3} m_2 l_2^2 \ddot{\theta}_2 + \frac{m_2 l_1 l_2 \ddot{\theta}_1}{2}\cos(\theta_1 - \theta_2) - \frac{m_2 l_1 l_2 \dot{\theta}_1^2}{2}\sin(\theta_1 - \theta_2) + \frac{1}{2} m_2 g l_2 \sin\theta_2 \quad (18)$$

Since, the model of the system can be represented as a double pendulum; the equation of motion can be formally represented as [14]

$$M(\theta)\ddot{\theta} + C\left(\theta, \dot{\theta}\right)\dot{\theta} + G(\theta) = \tau \quad (19)$$

where $\theta, \dot{\theta}, and\ \ddot{\theta}$ represent the angular positions, velocities, and accelerations of joints respectively; $M(\theta)$ is 2×2 inertia matrix; $C\left(\theta, \dot{\theta}\right)\dot{\theta}$ is 2×1 vector of Coriolis; $G(\theta)$ is 2×1 vector of gravitational torques; and τ is 2×1 vector of actuator joint torques. The inertia matrix, Coriolis vector and the vector of gravitational torques can be expressed as

$$M(\theta) = \begin{bmatrix} \frac{(m_1+3m_2)}{2} l_1^2 & \frac{m_2 l_1 l_2}{2}\cos(\theta_1 - \theta_2) \\ \frac{m_2 l_1 l_2}{2}\cos(\theta_1 - \theta_2) & \frac{m_2}{3} l_2^2 \end{bmatrix} \quad (19a)$$

$$G(\theta) = \begin{bmatrix} \frac{(m_1+2m_2)}{2} g l_1 \sin\theta_1 \\ \frac{m_2}{2} g l_2 \sin\theta_2 \end{bmatrix} \quad (19b)$$

$$C(\theta) = \begin{bmatrix} 0 & \frac{m_2 l_1 l_2 \dot{\theta}_2}{2}\sin(\theta_1 - \theta_2) \\ \frac{m_2 l_1 l_2 \dot{\theta}_1}{2}\sin(\theta_1 - \theta_2) & 0 \end{bmatrix} \quad (19c)$$

$$\tau = \begin{bmatrix} \tau_1 \\ \tau_2 \end{bmatrix},$$

From Eqs. (17) and (18), $\ddot{\theta}_1$ and $\ddot{\theta}_2$ can be obtained as

$$\ddot{\theta}_1 = \frac{K_4(\tau_1 - K_2\dot{\theta}_2^2 \sin(\theta_1-\theta_2) - K_3 \sin\theta_1) - K_2 cos(\theta_1-\theta_2)(\tau_2 - K_2\dot{\theta}_1^2 \sin(\theta_1-\theta_2) - K_5 \sin\theta_2)}{K_1K_4 - K_2^2 \cos(\theta_1-\theta_2)^2} \quad (20)$$

$$\ddot{\theta}_2 = \frac{K_1(\tau_2 - K_2\dot{\theta}_1^2 \sin(\theta_1-\theta_2) - K_5 \sin\theta_2) - K_2 cos(\theta_1-\theta_2)(\tau_1 - K_2\dot{\theta}_2^2 \sin(\theta_1-\theta_2) - K_3 \sin\theta_1)}{K_1K_4 - K_2^2 \cos(\theta_1-\theta_2)^2} \quad (21)$$

where [14],

$K_1 = \frac{(m_1+4m_2)}{4}\ l_1^2$, $K_2 = \frac{m_2 l_1 l_2}{2}$, $K_3 = \frac{(m_1+2m_2)}{2}\ g l_1$, $K_4 = \frac{m_2}{4}\ l_2^2$, $K_4 = \frac{m_2}{2}\ g l_2$

Table 1 lists the system parameters.

Table 1. The parameters of the system [16].

Parameter	Value	Unit
m_1, m_2	0.1	Kg
l_1, l_2	0.55	m
g	9.81	m/s^2

Assume the state variables are

$x_1 = \theta_1$: The angular position for the upper link.

$x_2 = \theta_2$: The angular position for the lower link.

$x_3 = \dot{x}_1$: The angular velocity for the upper link.

$x_4 = \dot{x}_2$: The angular velocity for the lower link.

Therefore [14],

$$\dot{x}_1 = x_3$$

$$\dot{x}_2 = x_4$$

$$\dot{x}_3 = \frac{K_4(\tau_1 - K_2 x_4^2 \sin(x_1-x_2) - K_3 \sin x_1) - K_2 cos(x_1-x_2)(\tau_2 - K_2 x_3^2 \sin(x_1-x_2) - K_5 \sin x_2)}{K_1K_4 - K_2^2 \cos(x_1-x_2)^2}$$

$$\dot{x}_4 = \frac{K_1(\tau_2 - K_2 x_3^2 \sin(x_1-x_2) - K_5 \sin x_2) - K_2 cos(x_1-x_2)(\tau_1 - K_2 x_4^2 \sin(x_1-x_2) - K_3 \sin x_1)}{K_1K_4 - K_2^2 \cos(x_1-x_2)^2} \quad (22)$$

The inputs are

$u_1 = \tau_1$: The external torque at the actuator of the upper link.

$u_2 = \tau_2$: The external torque at the actuator of the lower link.

The outputs are:

$y_1 = \theta_1$: The angular position for the upper link.

$y_2 = \theta_2$: The angular position for the lower link.

2.1. H_2PID controller design

In this paper, the full state feedback H_2 controller and PID controller have been used to robustly stabilize the system and track the desired trajectory for human walking swing system. Moreover, the ability of the control system to tolerate

disturbances and uncertainties has been tested. It is worth to mention, the control design was in two steps; the first step is by designing a full state feedback H_2 controller to achieve the required stabilizing, while in the second step the H_2 controller has been fused with dual PID controllers to enhance the performance of the system. Furthermore, the adjust culture algorithm (CA) has been used to find the optimal parameters of the proposed hybrid controller.

Recently, the significance of robust control in the topics of control systems becomes the most interesting subject for scientists. It can be considered the full state feedback H_2 controller as an optimal control algorithm. Figure. 2 shows the structure of the full state feedback controller [17]. The structure has two inputs and two outputs that mean the structure is MIMO which is represented by the matrix in Eq. (23) M. Uncontrolled input of the system, the control signal, the error signal, and the output of the system can be represented by the variables d, u,e, and y respectively [17].

$$M = \begin{bmatrix} A & B_1 & B_2 \\ C_1 & 0 & D_{12} \\ 1 & 0 & 0 \end{bmatrix} Kc \tag{23}$$

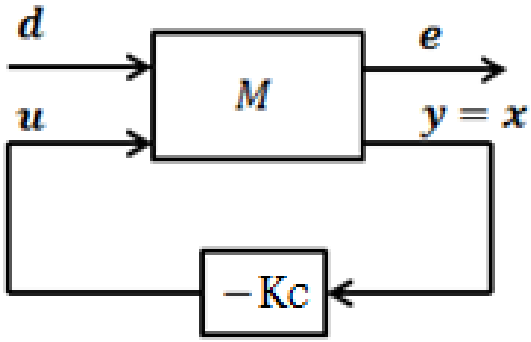

Fig. 2. A full state feedback H_2 control structure [17].

Assume that:

1-(A, B_1) and (A, B_2) are stabilizable.

2-(C_1, A) is detectable.

Now, by considering the system shown in Fig. 2, the system can be represented by

$$\dot{x} = Ax + B_1 d(t) + B_2 u(t)$$

$$e(t) = C_1 x(t) + D_{12} u(t)$$

$$y(t) = x(t) \tag{24}$$

And the transfer function of the closed-loop for H_2 (T_{ed}) is:

$$\|T_{ed}\|_{H_2}^2 = E(e^T(t)e(t)) \tag{25}$$

where

$$e^T e = x^T C_1^T C_1 x + 2x^T C_1^T D_{12} u + u^T D_{12}^T D_{12} u \tag{26}$$

To minimize Eq. (26), it is assumed that

$Q_f = C_1^T C_1$, $N_f = C_1^T D_{12}$ and $R_f = D_{12}^T D_{12}$

Then, the law of optimal state feedback is given by

$$u = -K_c x \tag{27}$$

where

$$K_c = R_f^{-1}(PB_2 + N_f)^T \tag{28}$$

The matrix P can be determined by applying the following Ricatti equation [17, 18]:

$$P\left(A - B_2 R_f^{-1} N_f^T\right) + \left(A - B_2 R_f^{-1} N_f^T\right)^T P - PB_2 R_f^{-1} B_2^T P + Q_f = 0 \tag{29}$$

The most common controller used in industry and academic research is the PID controller. The control signal $u(t)$ can be represented as:

$$u(t) = K_p e(t) + K_i \int_0^t e(t)d(t) + K_d \frac{d}{dt} e(t) \tag{30}$$

where $K_p, K_i,$ and K_d represent the parameters of the PID controller [19].

2.2. Controller parameters tuning

The Cultural Algorithm (CA) is one of the effective optimization algorithms which has been used in this research to find the proposed controller's parameters. Cultural evolution process represents the base of cultural algorithm [20]. There are two levels to evolution the process: micro and macro evolutionary levels. At the micro evolutionary level, the behavioural traits of individuals can be described socially as acceptable or unacceptable. At macro evolutionary level, the ability of individuals can generate their experience to the next generation [21]. The CA is known as dual inheritances evolutionary tend to consist from a population and a belief space. The belief space use to solve a problem from the population. Therefore, the process of evolutions can be used to direct in population and the acquired knowledge will save in belief space [20, 21]. The interaction between spaces is designed according to the following steps [21].

Step 1: For each parameter select an initial population of p candidate solutions, from a uniform distribution with has given domain from 1 to n.

Step 2: By objective function f assess the performance of each parent.

Step 3: The belief space can be initialized with candidate solutions and the problem domain.

Step 4: By applying a variation operator (V) generate p new offspring solutions. Now, there are 2 p.

Step 5: By objective function f assess the performance of each offspring solutions.

Step 6: From the population of size 2 p select randomly c competitions for each individual.

Step 7: Select the greatest p solutions to be parents for the next generation.

Step 8: By accepting individuals and acceptance function update the belief space.

Step 9: Unless an acceptable solution has been found or the available time is exhausted go back to step 4.

The following optimization targets were formulated to design an optimal H_2PID controller with the following requirements:

i. Minimization of the error signal $e(t)$.
ii. Minimization of the H_2 cost function characterized by a suitable tuning of Q_f and R_f matrices.
iii. Maximization of the system gain margin and Phase margin.

The above requirements can be combined in a single constraint to construct a new performance index for the proposed H_2PID controller. This performance criterion can be expressed by:

$$J(h) = \int_0^{t_f} e(t)^2 dt + \|T_{ed}\|_{H_2}^2 + (G.M)^{-1} + (P.M)^{-1} \quad (31)$$

where h represents a vector of the parameters to be optimized for the controller design. This vector can be defined as

$$h = [q_{11}\, q_{22}\, q_{33}\, q_{44}\, r_{11}\, r_{22} n_{11} n_{22}\, k_{p1}\, k_{i1}\, k_{d1}\, k_{p2}\, k_{i2}\, k_{d2}] \quad (32)$$

where

$$Q_f = \begin{bmatrix} q_{11} & 0 & 0 & 0 \\ 0 & q_{22} & 0 & 0 \\ 0 & 0 & q_{33} & 0 \\ 0 & 0 & 0 & q_{44} \end{bmatrix}, R_f = \begin{bmatrix} r_{11} & 0 \\ 0 & r_{22} \end{bmatrix}, \text{and } N_f = \begin{bmatrix} n_{11} & 0 \\ 0 & n_{22} \\ 0 & 0 \\ 0 & 0 \end{bmatrix}$$

and $k_{p1}\, k_{i1}\, k_{d1}$ represent the PID_1 controller parameters and $k_{p2}\, k_{i2}\, k_{d2}$ represent the PID_2 controller parameters. It is important to refer that the values of the elements $(q_{11}, q_{22}, q_{33}, q_{44})$ and (n_{11}, n_{22}) have a significant effect on the performance.

Figure. 3 shows the overall block diagram of the proposed H_2PID controller with CA algorithm.

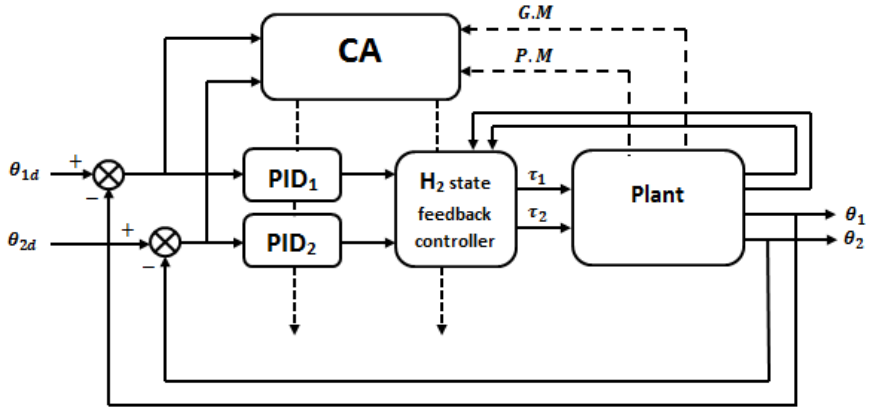

Fig. 3. The overall block diagram for the proposed controlled system.

3. Results and Discussion

By using Jacobean's method, the nonlinear system represented by Eq. (22) can be linearized with the equilibrium points listed in Table 2.

Table 2. The system equilibrium points [14].

Equilibrium points	Value	Unit
x_1	10	deg
x_2	20	deg
$\dot{x}_1$	0.3	rad/s
$\dot{x}_2$	0.4	rad/s
τ_1	0.5	$N.m$
τ_2	0.5	$N.m$

The resulting state space model is

$$\dot{x} = \begin{bmatrix} 0 & 0 & 1 & 0 \\ 0 & 0 & 0 & 1 \\ -18.9615 & 2.8818 & -0.2155 & -0.1274 \\ 20.2204 & -23.9035 & 0.6116 & 0.1796 \end{bmatrix} x + \begin{bmatrix} 0 & 0 \\ 0 & 0 \\ 49.2616 & -69.4362 \\ -69.4362 & 197.0466 \end{bmatrix} u$$

$$y = \begin{bmatrix} 1 & 0 & 0 & 0 \\ 0 & 1 & 0 & 0 \end{bmatrix} x + \begin{bmatrix} 0 & 0 \\ 0 & 0 \end{bmatrix} u \tag{33}$$

where the variables x and $\dot{x}$ represent the state vector and differential equation respectively, y represents the output equation.

In this section, the proposed controller is verified by applying it to the nonlinear human walking swing leg system (HWSS) model. Figure. 4 illustrates the behavior of the system before applying the controller. The angular positions for the hip and knee joints are exhibited for open loop and closed loop system. It is clear from Fig. 4 that the responses of the system are critical with high oscillation when the system is subjected to a step input.

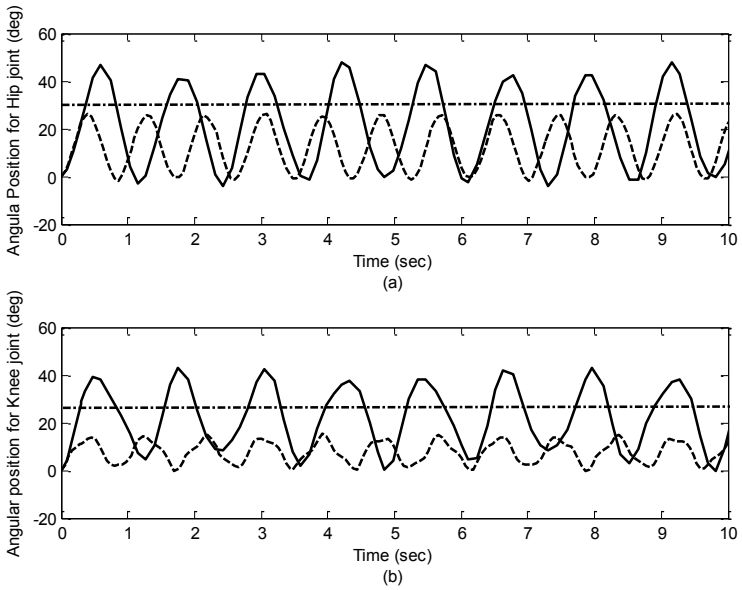

Fig. 4. Open loop and closed loop responses (a) hip joint (b) knee joint (Solid line represents open loop response, Dash line represents closed loop response, and Dash dot line represents the input).

To apply the H_2 state feedback controller to HWSS, the weighting matrices parameters have been obtained using CA algorithm as shown in Table 3.

Table 3. H_2 controller parameters.

Parameter	Value
q_{11}	900.121
q_{22}	600.041
q_{33}	100.221
q_{44}	100.114
r_{11}	1.111
r_{22}	1.223
n_{11}	2.157
n_{22}	2.192

The resulting K_c matrix is

$$K_c = \begin{bmatrix} 29.5583 & -0.1864 & 10.1104 & 0.0389 \\ -0.0826 & 24.3130 & 0.0312 & 10.0221 \end{bmatrix}$$

Figure 5 shows the responses of angular position and angular velocity for the hip and knee joints when H_2 controller has been applied on the system in case of stabilization. Demonstrated in Fig. 5, the proposed controller successfully stabilized the system in less than 2 seconds. Thus, the system has become internally stable.

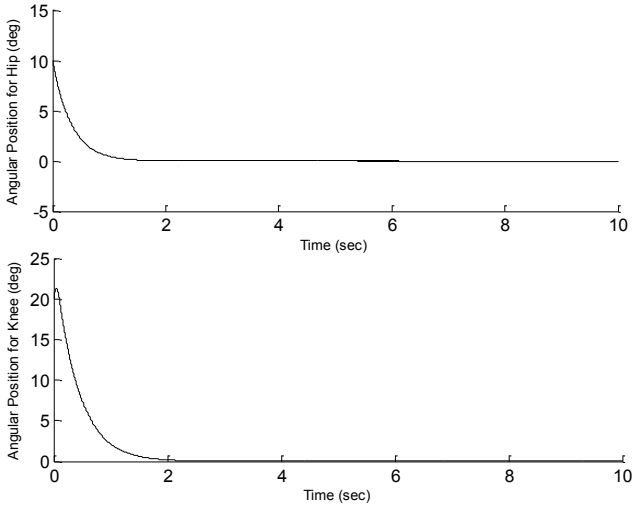

Fig. 5. Responses of angular positions for hip and knee joints in case of stabilization with H_2 controller.

Figure 6 shows the time responses after applying the full state feedback H_2 controller to the system in case of tracking with desired inputs, for $\theta_1 = 30°$ and $\theta_2 = 15°$. However, it is clear to see that the responses have steady-state error. This indicates that the H_2 full state feedback controller cannot entirely compensate for the generated errors and its performance is limited. Moreover, the control actions tend to

have a large initial torques spike which is unacceptable behaviour of system actuators, as shown in Fig. 7.

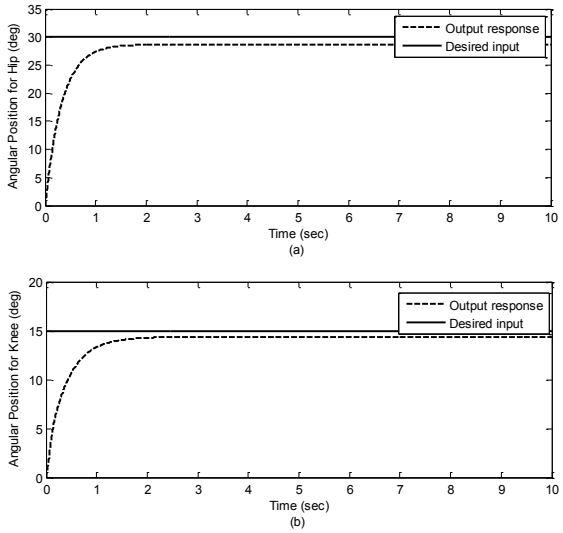

Fig. 6. The time response with H_2 controller in case of tracking (a) hip joint (b) knee joint.

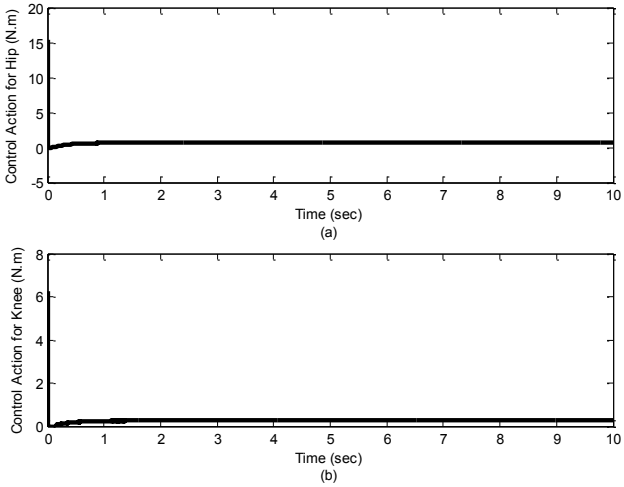

Fig. 7. Control action signals in case of H_2 controller (a) hip joint (b) knee joint.

The cultural algorithm is a newly introduced optimization method with proven capabilities in finding the optimal values of various applications. Based on the literature, many comparisons have been made to ensure the superiority of this method over other optimization algorithms. The CA algorithm is used to obtain the optimal parameters of controller that give the desired performance. The CA parameters values that have been used to find the best values for the parameters of the controller are shown in Table 4.

Table 4. CA parameters values.

Parameter Name	Value
Number of decision variables	12
Decision variables lower bound	0.1
Decision variables upper bound	1000
Maximum number of iterations	50
Population size	40
Acceptance ratio	0.35
Alpha	0.3
Beta	0.5

Figure. 8 shows the evaluation of the best cost function value over iterations calculated from the cultural optimization algorithm to find the optimal parameters of the H_2PID controller. It is shown that the settings for CA parameters listed in Table 4 were adequate for this application. It can be seen that increasing the number of iteration above 25 did not improve the convergence of CA significantly.

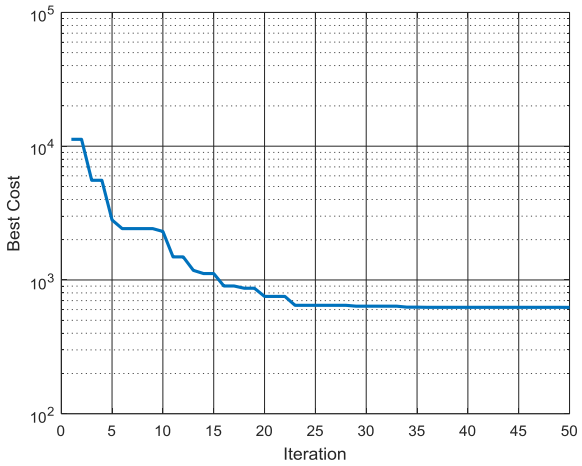

Fig. 8. Best cost vs. iteration.

The optimized parameters of the proposed controller are listed in Table 5.

Table 5. H_2PID controller parameters.

2	Value
q_{11}	846.5
q_{22}	286.2
q_{33}	100
q_{44}	475.7
r_{11}	405.4
r_{22}	279.1
K_{p1}	20.4359
K_{i1}	15.2093
K_{d1}	2.9336
K_{p2}	8.909
K_{i2}	17.5203
K_{d2}	1.3817

The resulting state feedback gain matrix is

$$K_c = \begin{bmatrix} 0.50021 & -0.44802 & 0.20723 & -0.36633 \\ 0.23001 & 0.93752 & 0.06505 & 1.2758 \end{bmatrix}$$

Figure. 9 shows the responses of angular positions for the hip and knee joints when the proposed controller has been applied on the system in case of tracking. It can be seen that the responses for hip and knee are stable with zero steady-state error. The settling time has been significantly reduced without overshooting the desired angles set. Moreover, the proposed controller has a less aggressive control action for hip and knee joints while maintaining an applicable range, as shown in Fig. 10.

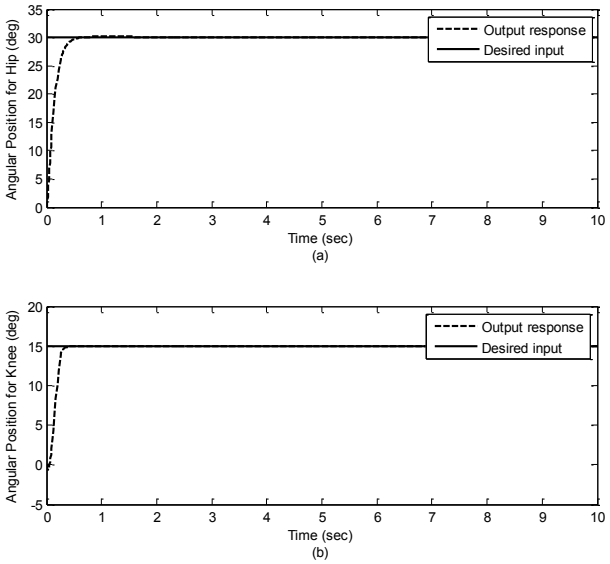

Fig. 9. The time response with the H_2PID. controller in case of tracking (a) hip joint (b) knee joint.

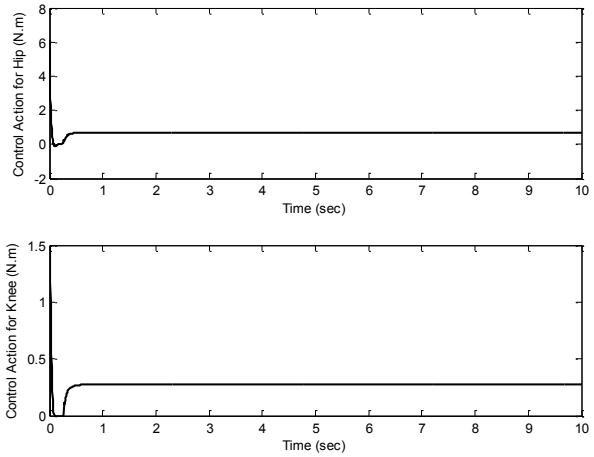

Fig. 10. Control action for hip and knee joints in case of tracking.

On the other hand, the tracking performance of the controlled system for a given trajectory input signal is shown in Fig. 11. It can be seen that the controlled system can effectively track the given trajectory. This can be attributed to the high ability of the proposed H_2PID controller in improving the tracking properties.

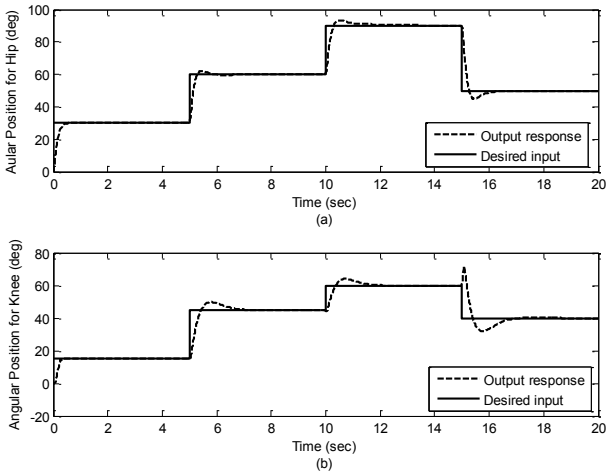

Fig. 11. Tracking properties of the controlled system with H_2PID controller (a) hip joint (b) knee joint.

The robustness of the controlled system is then tested twice with two cases. The first test was when a disturbance signal was subjected to the system. The value of disturbance was 15% of the reference input and it was applied at $t = 4\ s$. Figure. 12 shows the effect of disturbance on the output of angular positions for hip and Knee joints and how the controller can effectively reject these disturbances holding the system to its steady-state value. Figure. 13 shows the behavior of the control action, it is clear from Fig. 13 that the control actions acted to reject the disturbance and maintain stability with minimal energy. It is shown that a low control effort was needed after applying the disturbance. This can be attributed to the extra torque given by the applied disturbance.

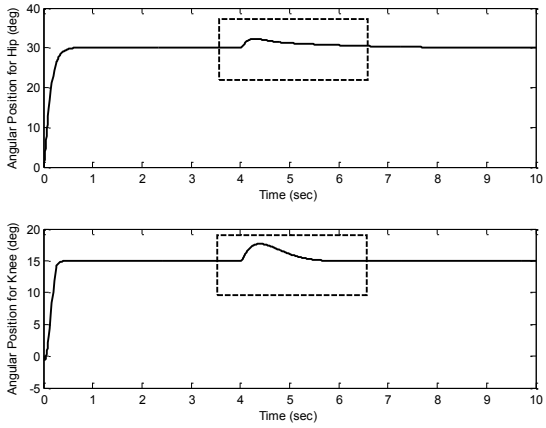

Fig. 12. Disturbance rejection properties of the controlled system.

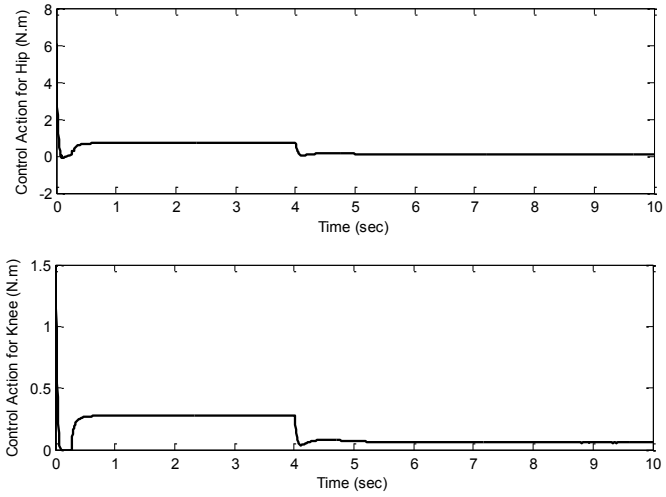

Fig. 13. Control action for hip and knee joints when the disturbance is applied.

The second test of robustness is done with applying $\pm 10\%$ variation in system parameters(m_1, m_2, l_1, l_2). Figure. 14(a) shows the responses of angular position for hip joint while Fig. 14(b) shows the responses of angular position for knee joint. It can be observed that the proposed controller has the capacity to compensate the system parameters variation and achieve the desired performance. It is worth noting that, these robustness properties are inherited from the PID controller part of the design.

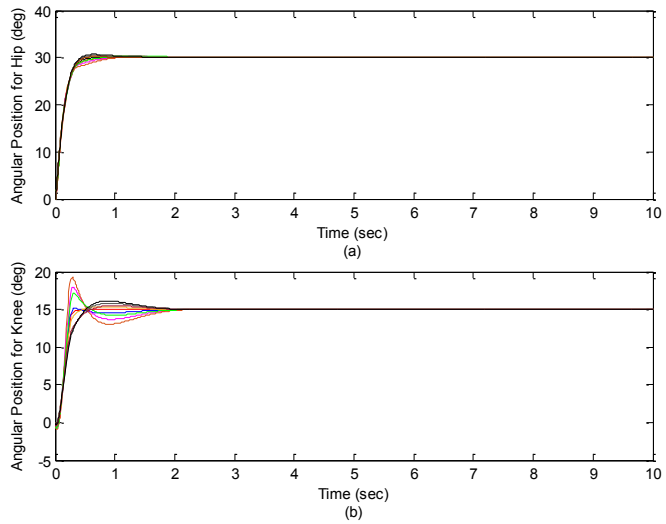

Fig. 14. The responses of angular position for joints with the system parameters variation (a) hip joint (b) knee joint.

A comparison between the proposed H_2PID controller and Mixed H_2/Sliding Mode controller [12] for human swing leg system has been given to show the effectiveness of

the proposed controller. Table 6 presents a comparison between H_2PID controller and Mixed H_2/Sliding Mode controller in terms of time response specifications.

Table 6. Performance comparison.

Controller	Hip joint		Knee joint	
	t_r (s)	t_s (s)	t_r (s)	t_s (s)
Mixed H_2/SMC [12]	3	4	1	2
H_2PID	0.3	0.5	0.5	0.25

From Table 6 it is seen that the proposed H_2PID controller can achieve a more desirable performance in comparison to the Mixed H_2/SMC proposed by [12]. This can be seen in terms of achieving small rise time and settling time. Also, the control action does not suffer from chattering which is one of the features of sliding mode control.

4. Conclusions

In this paper, the hybrid H_2PID controller was proposed to robustly stabilize the system and achieve desirable tracking properties. It was shown that combination between H_2 and PID controller can give a better performance than if one of them is used. The PID controller was added to enhance the tracking properties where the H_2 control was unable to give an adequate time response specifications. The CA algorithm was used as an effective optimization method to optimize the controller design procedure. The results showed that the proposed controller can robustly stabilize the system with more desirable performance.

Nomenclatures

$e(t)$	Error signal
g	Acceleration of gravity, m^2/s
$G.M$	Gain margin, db
h_1	Heights of the center mass for thigh, m
h_2	Heights of the center mass for shank, m
I_1	Thing moment of inertia, kg m^2
I_2	Shank moment of inertia, kg m^2
k_e	Kinematic energy, J
L	Lagrange Dynamics
l_1	Length of the thigh, m
l_2	Length of the shank, m
m_1	Mass of the thigh, kg
m_2	Mass of the shank, kg
$P.M$	Phase margin, deg
P_e	Potential energy of the system
v_2	Linear velocity for shank, m/s

Greek Symbols

θ_1	Rotation angle for the hip joint, deg
θ_2	Rotation angle for the knee joint, deg
τ_1	External torques applied on the thigh, N. m
τ_2	External torques applied on the shank, N. m

Abbreviations

ANN	Adaptive Neural Network
CA	Cultural Algorithm
CPG	Central Pattern Generator
DSP	Double Support Phase
HWSS	Human Walking Swing leg System
MCIWO	Modified Chaotic Invasive Weed Optimization
MPC	Model Predictive Control
NNPC	Neural Network Predictive Control
SIDP	Self-Impact Double Pendulum
SSP	Single Support Phase

References

1. Bazargan-Lari, Y.; Eghtesad, M.; Khoogar, A.; and Mohammad-Zadeh, A. (2015). Tracking control of a human swing leg as a double-pendulum considering self-impact joint constraint by feedback linearization Method. *Journal of Control Engineering and Applied Informatics*, 17(1), 99-110.
2. Bazargan-Lari, Y.; Gholipour, A.; Eghtesad, M.; Nouri, M.; and Sayadkooh, A. (2011). Dynamics and control of locomotion of one leg walking as self-impact double pendulum. *IEEE 2nd International Conference on Control, Instrumentation and Automation (ICCIA),* Shiraz, Iran, 201-206.
3. Andreas, D.; and Carl, S. (2009). Comparative study of numerical methods for optimal control of a biomechanical system controlled motion of a human leg during swing phase. Master's Thesis, Department of Applied Mechanics, Division of Dynamics, Division of Material and Computational Mechanics, Göteborg, Sweden.
4. Zhang, J.; Shen, L.; Shen, L.; and Li, A. (2010). Gait analysis of powered bionic lower prosthesis. *IEEE International Conference on Robotics and Biomimetics (ROBIO)*, Tianjin, China, 25–29.
5. Wang, L.; Van Asseldonk, E.H.; and Van der Kooij, H. (2011). Model predictive control-based gait pattern generation for wearable exoskeletons. *IEEE International Conference on Rehabilitation Robotics*, Zurich, Switzerland, 1-6.
6. Deisenroth, M.P.; Calandra, R.; Seyfarth, A.; and Peters, J. (2012). Toward fast policy search for learning legged locomotion. *IEEE/RSJ International Conference on Intelligent Robots and Systems (IROS),* Vilamoura, Portugal, 1787–1792.
7. Desai, R.; and Geyer, H. (2012). Robust swing leg placement under large disturbances. *IEEE International Conference on Robotics and Biomimetics (ROBIO)*, Guangzhou, China, 265–270.
8. Bazargan-Lari, Y.; Eghtesad, M.; Khoogar, A.R.; and Mohammad-Zadeh, A. (2015). Adaptive neural network control of a human swing leg as a double-pendulum considering self-impact joint constraint. *Transactions of the Canadian Society for Mechanical Engineering*, 39(2), 201-219.
9. Ekkachai, K.; and Nilkhamhang, I. (2016). Swing phase control of semi-active prosthetic knee using neural network predictive control with particle swarm optimization. *IEEE Transactions on Neural Systems and Rehabilitation Engineering*, 24(11), 1169-1178.

10. Mandava, R.K.; and Vundavilli, P.R. (2019). An optimal PID controller for a biped robot walking on flat terrain using MCIWO algorithms. *Evolutionary Intelligence*, 12(1), 33-48.
11. Wang, B.; Wan, Z.; Zhou, C.; Wu, J.; Qiu, Y.; and Gao, Z. (2019). A multi-module controller for walking quadruped robots. *Journal of Bionic Engineering*, 16(2), 253-263.
12. Ali, H. I.; and Kadhim, M.J. (2018). Mixed h2/sliding mode controller design for human swing leg system. *IEEE Third Scientific Conference of Electrical Engineering (SCEE)*, Baghdad, Iraq, 156-161.
13. Gregg, R.D.; Lenzi, T.; Hargrove, L.J.; and Sensinger, J.W. (2014). Virtual constraint control of a powered prosthetic leg: From simulation to experiments with transfemoral amputees. *IEEE Transactions on Robotics*, 30(6), 1455-1471.
14. Ali, H.I.; and Abdulridha, A.J. (2018). State feedback sliding mode controller design for human swing leg system. *ALNAHRAIN Journal for Engineering Sciences*, 21(1), 51-59.
15. Singh, S.; Mukherjee, S.; and Sanghi, S. (2008). Study of a self-impacting double pendulum. *Journal of Sound and Vibration*, 318(4-5), 1180-1196.
16. Liang, C.; Ceccarelli, M.; and Takeda, Y. (2008). Operation analysis of a one-DOF pantograph leg mechanisms. *Proceedings of the 17th International Workshop on Robotics in Alpe-Adria-Danube* (*RAAD*) *Region,* Ancona, Italy, 17, 1–10.
17. Sinha, A. (2007). *Linear Systems: optimal and robust control*. CRC press, Taylor and francis Group.
18. Ali, H.I. (2018). *Swarm Intelligence to Robust Control Design,* USA, United Scholars.
19. Hasan, A.; Hussain, B.K.; Alzubaidi, L.; and El-Gizawy, A. (2017). Developing semiautonomous system for robust performance of centrifugal pumping system. IEEE *Annual Conference on New Trends in Information & Communications Technology Applications* (*NTICT*), 310-315.
20. Chung, C.J.; and Reynolds, R.G. (1996). A testbed for solving optimization problems using cultural algorithms. *Evolutionary Programming*, 225-236.
21. Coello, C.A.C.; and Becerra, R.L. (2002). Adding knowledge and efficient data structures to evolutionary programming: A cultural algorithm for constrained optimization. *Proceedings of the 4th Annual Conference on Genetic and Evolutionary Computation*, New York City, New York, 201-209.